Surface Science 692 (2020) 121516

Contents lists available at ScienceDirect

Surface Science

journal homepage: www.elsevier.com/locate/susc

Room temperature oxidation of GaAs(110) using high translational kinetic energy molecular beams of O_2 visualized by STM

Tim Grabnic[1], Ross Edel[1], S.J. Sibener*

The James Franck Institute and Department of Chemistry, The University of Chicago, 929 East 57th Street, Chicago, IL 60637, United States

ARTICLE INFO

Keywords:
Gallium arsenide
Molecular beams
STM
Oxidation
Interfacial reaction kinetics

ABSTRACT

This study examines the reactive surface dynamics of GaAs(110) oxidation with molecular oxygen at room temperature over a range of impinging kinetic energies. Visualization of the surface by scanning tunneling microscopy (STM) after exposures to O_2 with kinetic energies of 0.4–1.2 eV provides morphological and kinetic data that were obtained utilizing a novel instrument that combines a supersonic molecular beam with an in-line, *in-situ* STM. Oxidation was found to proceed by two morphologically distinct, competing mechanisms: a spatially homogeneous process with randomly distributed chemisorbed oxygen atoms leading to layer-by-layer oxide growth, and a spatially heterogeneous process with oxides nucleating on structural surface defects and growing vertically and laterally with continued exposure. Both oxidation mechanisms exhibit enhanced reactivity with increasing kinetic energy. Only trace oxidation was observed with O_2 kinetic energies below 0.7 eV; a rapid increase in the rate of oxidation from 1.0 to 1.2 eV was found with homogeneous and heterogeneous oxidation proceeding simultaneously until full surface coverage was reached. In addition, the relative rates of the two mechanisms appear to change with O_2 kinetic energy: spatially homogeneous oxidation is expected to dominate at lower kinetic energies (<0.7 eV) while the heterogenous growth of oxide islands increasingly dominates with higher kinetic energies (≥ 1.0 eV). The results obtained in this study conclusively demonstrate that a heterogenous oxidation mechanism is activated on GaAs(110) at high O_2 kinetic energies, and reveal that thin oxide layers can be achieved with higher efficiency at room temperature using molecular beams of oxygen. These results provide vital information about the morphological evolution of the surface in conjunction with the overall kinetics, and identify a controlled method of enhanced oxidation at moderate temperatures that could potentially improve abruptness at oxide interfaces and be used in the fabrication of GaAs semiconductor devices.

1. Introduction

III-V compound semiconductors may be the key to developing ever-faster electronic devices as silicon transistors reach their size limitations [1]. GaAs represents one of the most promising semiconductor materials due to an electron mobility five times that of silicon and a high radiation hardness valuable in aerospace and military applications such as integrated circuits and solar cells for spacecraft [2]. The performance and quality of gallium arsenide metal-oxide-semiconductor (MOS) devices depends critically on the ability to create ultra-thin oxide films on the substrate surface. Previous studies [3–10] on the oxidation of the GaAs substrate have utilized aggressive conditions involving high-temperature or electrochemical environments to overcome the low reactivity of O_2 on GaAs under ambient conditions [11,12]. Ideally, enhancement of GaAs oxidation could be achieved using relatively low surface temperatures and clean environments to maintain surface stoichiometry and reduce defects in the oxide film. A fundamental understanding of the O_2-GaAs interface is therefore required to probe new oxidation pathways of the GaAs surface and to ultimately improve the processing and manufacturing of GaAs MOS devices.

In this paper, we present a marked enhancement of oxidation kinetics on the *p*-type GaAs(110) surface using impinging O_2 with high kinetic energies and incident angles oriented normal or 45° to the surface. We have utilized a unique approach to studying interfacial reaction dynamics by visualizing the oxidation of a *p*-type GaAs(110) surface at room temperature with energy- and angle-selected O_2 using a combination of supersonic molecular beam and ultra-high vacuum scanning tunneling microscopy (STM) techniques. This experimental approach has been used previously to successfully answer questions about the site-specific reactivity of O_2 on Si(111)-7×7 [13] and

* Corresponding author.
E-mail address: s-sibener@uchicago.edu (S.J. Sibener).
[1] TG and RE contributed equally to this work and are co-first authors of this manuscript.

https://doi.org/10.1016/j.susc.2019.121516
Received 26 August 2019; Received in revised form 21 October 2019; Accepted 26 October 2019
Available online 30 October 2019
0039-6028/

HOPG [14] surfaces. The combination of supersonic molecular beam and STM techniques links time-evolving morphologies to reaction kinetics, providing spatio-temporal correlations that govern the reactivity of surface reactions. By visualizing micrometer to sub-nanometer length-scales over time as oxidation proceeds, we have monitored the oxidation process from its initial phases to the formation of large-scale oxides on the surface. These results demonstrate two simultaneous oxidation mechanisms with distinct spatial distributions: the homogenous accumulation of randomly dispersed chemisorbed oxygen atoms as well as the heterogenous nucleation of oxide islands near defects.

Molecular oxygen starts to dissociatively chemisorb on the GaAs (110) surface at temperatures above 60 K [15]. The initial sticking coefficient for thermally dosed O_2 on a clean GaAs(110) surface is 2×10^{-5}, with oxygen initially adsorbing at a linear rate followed by a quasi-logarithmic uptake with continued exposure [12]. Results from AES and XPS studies indicate that the initial chemisorption ($\sim 3 \times 10^5$ L; 1 L = 10^{-6} Torr sec) of O_2 is slow and only increases the surface coverage to Θ = 0.05–0.1 depending on the amount of surface defects present [16]. The main oxygen uptake onto the surface proceeds *via* activated adsorption followed by field-assisted growth of an oxide phase [17–20]; the formation of subsurface oxides is still disputed [21–23]. Subsequent oxidation appears to be layer-by-layer [17,19] and has been described by the Mott-Cabrera mechanism [24], a phenomenon in which an electric field assists the oxidation process *via* electrons tunneling through the oxide film [20]. While the initial oxidation is generally assumed to be spatially homogeneous across the surface, there is some indication of spatially inhomogeneous oxidation with oxide islands nucleating on defects [21,22].

Numerous AES and photoemission studies [25–30] have addressed the bonding coordination of the adsorbed oxygen, with results indicating varying bonding geometries during different stages of the oxidation process. At high oxygen coverages, experimental [21–23] and theoretical evidence [31] indicates O atoms are multicoordinated about equally between Ga and As atoms. In the initial oxidation regime, conflicting evidence supports preferential bonding to surface As [26,32,33] and Ga [16,22,34,35] atoms, as well as bonding in bridge-bond positions with coordination to both Ga and As [28,36]. Experimental and theoretical studies on multiple GaAs(100) surfaces have demonstrated that the bonding of oxygen to surface Ga atoms is thermodynamically favored over bonding to surface As atoms [37–39].

STM imaging of the clean GaAs(110) surface exhibits atom-selective behavior in which positive sample biases with respect to the STM tip (unoccupied surface state imaging) visualize the Ga atoms while negative sample biases (occupied surface state imaging) visualize the As atoms [40]. Investigations using STM have demonstrated spatially homogeneous oxidation with the stochastic appearance of scattered oxidized sites on the GaAs(110) surface [36,41], while the spatially heterogenous nucleation and growth of oxide islands has also been observed by STM on the GaAs(100) surface [42]. The presence of spatially homogeneous chemisorbed oxygen atoms on a *p*-type GaAs (110) surface was found on defect-free terraces as shown by subsequent imaging in the same $\sim$225 nm^2 area after exposure, and the imaging suggests that the chemisorbed oxygen sits in an interchain bridging site aligned in the [1$\bar{1}$0] direction with respect to the surface As atoms [36]. The chemisorbed O atoms demonstrate slight variations in topographical height and width with changes in imaging conditions but always appear as small isolated protrusions on the surface with a lateral size of 4–6 Å at full-width half-maximum (FWHM) on a *p*-type sample. This differs significantly from the delocalized nature of oxygen adsorbates on an *n*-type sample that results from the negatively-charged nature of the chemisorbed O atom, as opposed to the neutral adsorbates on *p*-type samples [41,43]. Spatially heterogenous oxidation was observed on a *n*-type GaAs(100) surface, with nucleation centers growing to cover the surface in a manner similar to the oxidation mechanism found on InP [42,44]. 100 nm × 100 nm STM images of the surface with continued exposure to air revealed the nucleation of oxide islands, which grew laterally to cover the surface in a uniform oxide layer $\sim$2 nm thick. This stands in contrast with previous findings indicating that GaAs oxidation is homogenous across the surface and proceeds layer-by-layer.

The results of this paper will detail the reactive oxidation of a GaAs (110) sample at room temperature using high kinetic energy impinging O_2 while visualizing the corresponding morphological evolution of the surface during exposures. By employing a combination of molecular beam and STM techniques, we have explored the energetic barriers to reaction using monoenergetic O_2 and have illustrated two kinetically and morphologically distinct mechanisms of oxide growth: the heterogeneous nucleation and growth of oxide-islands at O_2 kinetic energies $\geq$1.0 eV, and the homogenous accumulation of randomly distributed oxidized sites leading to layer-by-layer oxide growth. Characterization of the kinetics and surface evolution of both modes of oxide formation will be detailed, and a comprehensive overview of the high kinetic energy oxidation of the GaAs(110) surface will be presented.

2. Experimental

The results reported here were obtained using a new UHV instrument combining supersonic molecular beam and STM/AFM techniques. The instrument is composed of a triply differentially pumped beamline, a surface preparation/characterization chamber, and an SPM chamber containing a variable temperature SPM based on the ultra-stable design of Shuheng Pan, built in collaboration with RHK. As described in previous publications [13,14], the custom-built Pan STM has been designed with the surface plane vertical such that the sample can be exposed to the supersonic molecular beam with the STM tip still in contact, and includes the capability for exploring variable angles of incidence. This unique configuration and the high stability of the microscope allow given nanoscopic areas to be revisited after exposure to the molecular beam, tracking the progression of surface oxidation over time.

Supersonic molecular beams were generated by the expansion of a 5% O_2/95% He gas mixture through a 30 μm molybdenum pinhole at pressures from 20 to 80 psi and nozzle temperatures ranging from 300 to 975 K (± 5%). The translational kinetic energy of the molecular beam at each nozzle temperature was measured using time-of-flight (TOF), and values of 0.38 ± 0.04 eV, 0.73 ± 0.08 eV, 0.97 ± 0.15 eV, 1.10 ± 0.12 eV, and 1.22 ± 0.17 eV were found for nozzle temperatures of 300, 575, 775, 875, and 975 K, respectively. The uncertainty values in these energies represent the FWHM of each energy distribution. The molecular beam flux for all beam conditions was on the order of 10^{13} O_2 molecules cm^{-2} s^{-1}, as determined by the King and Wells method [45]. The GaAs(110) sample was positioned in the SPM chamber during exposures, with a 4 mm diameter beam spot on the crystal. The sample was held at room temperature for all experiments and the surface plane was oriented either normal or at 45° with respect to the impinging beam. The kinetic energy of oxygen in each beam therefore exceeds the thermal energy of the room temperature surface by over an order of magnitude. Imaging was performed between beam exposures. Same-spot visualization experiments, whereby the same set of atoms could be revisited after exposure to high kinetic energy O_2, were completed by moving the STM tip laterally multiple micrometers downrange (away from the O_2 beam) from the reference area during each exposure to mitigate tip shadowing while keeping the tip in contact with the surface. The STM tip was then moved back to the reference area after the exposure and the set of reference atoms were located using topographical markers on the surface. Only areas of the sample with direct line of sight to the beam were reacted after exposure, confirming that thermalized O_2 reflected from the STM tip and/or chamber did not significantly affect the oxidation of the surface.

GaAs(110) crystals (*p*-type Zn-doped, VGF grown, MTI Corporation) were used for all experiments, and were cut into approximately 5 mm × 1 cm strips for appropriate fit onto the sample mounts.

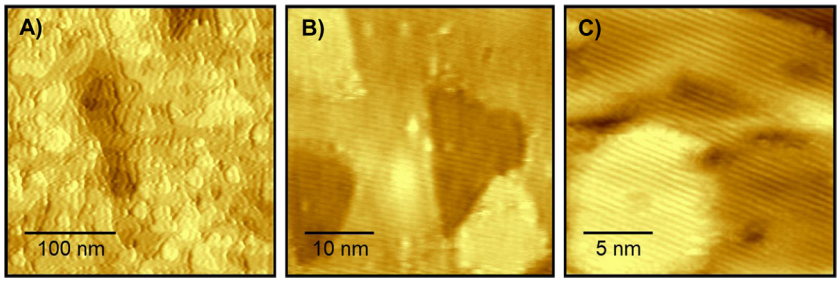

Fig. 1. A) 300 nm × 300 nm (−2.8 V, −0.6 nA), **B)** 40 nm × 40 nm (2.8 V, 0.6 nA), and **C)** 20 nm × 20 nm (−3.0 V, −0.3 nA) STM images of representative clean GaAs (110) surfaces obtained after multiple sputter/anneal cycles. The terrace sizes and overall roughness of the surface are illustrated in **A)**, while the row structure can be seen running horizontally (and slightly down moving left to right) across **B)** and **C)**, along with the presence of natural bright site defects.

Samples were cleaned in a UHV chamber ($<5 \times 10^{-11}$ Torr base pressure) by repeated cycles of ion sputtering at room temperature using 0.5–1.0 keV Ar^+ ions followed by subsequent annealing at 700 K ± 30 K to form the well-ordered GaAs(110) surface [46–48]. The surface was heated by applying current directly through the sample and the temperature was monitored using a Mikron infrared pyrometer ($\varepsilon = 0.69$) during the annealing process. An ion flux of ~7 μA/cm^2 was measured during the sputtering cycles. STM images were taken using etched or cut $Pt_{0.8}Ir_{0.2}$ tips.

3. Results and discussion section

A representative clean GaAs(110) surface as imaged by STM is shown in Fig. 1, which was achieved after multiple cycles of ion sputtering with 0.5–1.0 keV Ar^+ ions and subsequent annealing to ~700 K. Fig. 1A demonstrates both the overall terrace size and topography of the surface on a larger, mesoscopic scale. Fig. 1B and C illustrate the row structure on the terraces, along with individual bright site surface defects. The observed row structure in the nanoscopic images matches the expected periodicity of the GaAs(110) surface, scales appropriately with images of different sizes, and does not change with varying scanning conditions.

No significant oxidation was observed with exposures up to 6×10^{17} cm^{-2} using O_2 with kinetic energies of 0.4 eV, while 0.7 eV O_2 demonstrated only minimal surface oxidation. A critical threshold in reactivity was reached around 1.0 eV, as shown in Fig. 2. After this point, reactivity increased at a greater than linear rate with kinetic energy, reaching a value at 1.2 eV about four orders of magnitude higher than what has been observed previously with background exposure to room temperature oxygen [11]. The observed increase in reactivity is likely due in large part to the activation of the

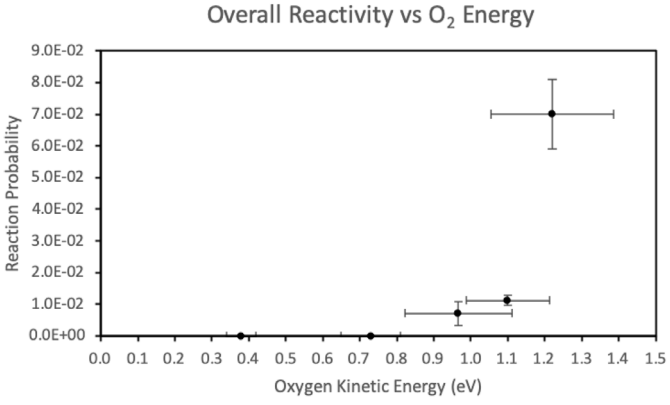

Fig. 2. Overall reaction probability vs O_2 kinetic energy for exposure to oxygen impinging normal to the surface with kinetic energies between 0.4 eV and 1.2 eV. Reactivity sharply increases after a critical threshold energy is reached between 0.7 eV and 1.0 eV, showing a nonlinear relationship between O_2 energy and reactivity. The horizontal error bars are derived from the TOF measurements at each beam energy to show the width of the distribution of O_2 kinetic energies.

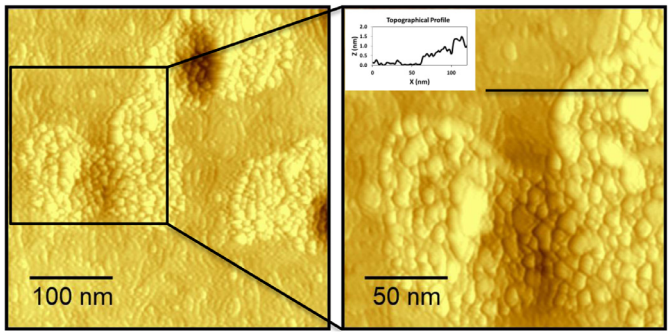

Fig. 3. A 400 nm × 400 nm STM image (−2.0 V, −0.6 nA) of an oxide island on a GaAs(110) surface after exposure to ~7×10^{16} cm^{-2} of 0.7 eV kinetic energy O_2 with a magnified image (200 × 200 nm; −2.0 V, −0.6 nA) showing a more detailed view of the same area. The topographical profile on the magnified image demonstrates the corrugation and height of the oxide island. Spatially heterogeneous oxidation creates patches of oxide that nucleate on surface defects, such as the pit shown here, and grow laterally to cover the surface with further oxygen exposure.

heterogenous oxidation mechanism with oxygen energies ≥0.7 eV. As shown in Fig. 3, STM imaging has revealed the nucleation and growth of "oxide islands" after exposure to ~7×10^{16} cm^{-2} of 0.7 eV O_2 normal to the surface that appear to nucleate on or near pit defects. The oxide islands have a height profile of ~5–10 Å above the surface with both positive and negative scanning bias, consistent with a thin oxide film [49,50]. The oxide islands completely replace the row structure seen on clean terraces and are morphologically distinct from the clean GaAs(110) surface. Given that the surface in all cases was dominated by such ~5–10 Å tall oxide islands, the reactivity shown in Fig. 2 was calculated by approximating the fully oxidized surface as consisting of a uniform 10 Å thick sheet of β-Ga_2O_3, as any As_2O_3 formed at the interface with GaAs is expected to react to form Ga_2O_3 and As [51]. This 10 Å thickness value represents an upper bound on the probable thickness of the oxide layer at full coverage. Reaction probability per impinging O_2 molecule, P, is then given by

$$P = \frac{3\ h\ N_A \rho_{Ga_2O_3}}{2\ M_{Ga_2O_3} \Phi_{O_2} t}$$

for oxide thickness $h = 10$Å, density $\rho_{Ga_2O_3}$, Avogadro's number N_A, molar mass $M_{Ga_2O_3}$, stoichiometric factor $\frac{3}{2}$, flux of impinging oxygen Φ_{O_2}, and time to fully oxidize the surface t. The reaction probability is therefore here defined as the ratio of the number of impinging O_2 molecules that contribute to the 10 Å thick oxide layer to the total fluence of O_2 molecules. This calculation allows a reasonable comparison of relative reactivities in order to determine the effect of impinging O_2 energy on the reactivity of the GaAs(110) surface.

Infrequent oxide islands grew to a maximum area on the order of 10^4 nm^2 with exposures up to 5×10^{17} cm^{-2} of 0.7 eV oxygen, and cumulatively covered a very small percentage of the surface. At higher energies (≥1.0 eV), the islands expanded laterally with continued exposure until they consumed the entire surface. In some cases, islands grew vertically as well as laterally, with STM visualization revealing the

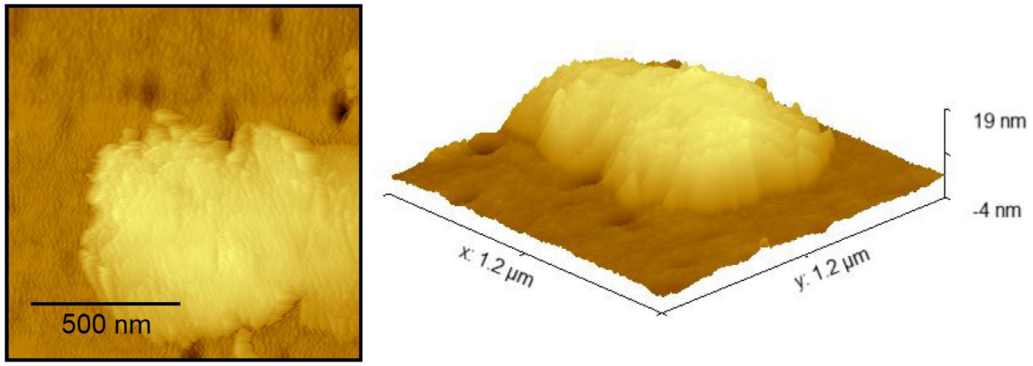

Fig. 4. A 1.2 μm × 1.2 μm image (−2.8 V, −0.6 nA) STM image of an elevated oxide island on a GaAs(110) surface formed after a total exposure of ~1 × 10^{17} cm^{-2} of O_2 with a kinetic energy of 1.0 eV. A 3D representation of the STM image is shown at right to emphasize the height and roughness of the oxide island. The high vertical elevation of such islands may indicate subsurface oxidation and "blistering" of the surface.

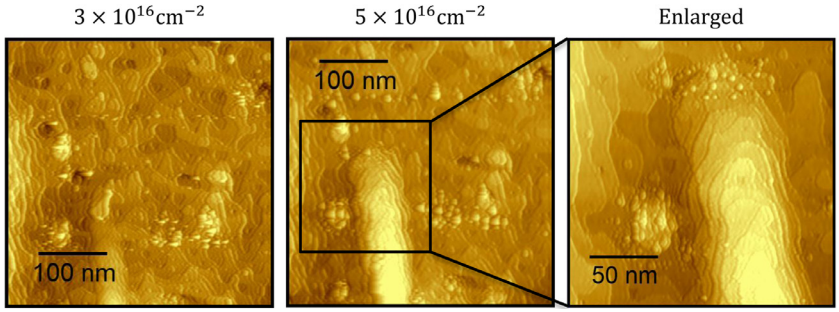

Fig. 5. Sequential STM images (−2.8 V, −0.6 nA) in the same local area illustrating the elevation of clean terraces on a room temperature GaAs(110) surface after exposure to 1.2 eV O_2 impinging 45° from normal to the surface. Two 400 nm × 400 nm images show the area after 3 × 10^{16} cm^{-2} O_2 exposure (left) and after 5 × 10^{16} cm^{-2} O_2 exposure (center). The morphological change is likely due to subsurface oxidation and subsequent lattice expansion resulting in the "blistering" of the surface. The magnified 200 nm × 200 nm image at right highlights the raised terraces seen in the middle image.

presence of tall, multilayer oxide islands spanning >1 μm in diameter, such as the one shown in Fig. 4. The dramatic vertical growth of these islands likely indicates multilayer/subsurface oxidation near intrinsic large-scale surface defects (*i.e.* microfissures, dislocations, *etc.*) as previously suggested in the literature [22], which then cause the surface to "blister" as a result of the lattice expansion resulting from the formation of subsurface Ga_2O_3 and/or As_2O_3. Fig. 5 shows the uplift of clean GaAs terraces after exposure to 1.2 eV oxygen, possibly as a result of subsurface oxidation. This area of the surface is adjacent to a large-scale surface defect, which comports with the idea that subsurface oxidation occurs through the exploitation of deep surface fissures. This blistering mechanism explains the vertical growth of the islands without the need for mass transport of gallium and arsenic atoms, which at room temperature would be too slow to represent a realistic possibility.

Using our unique ability to monitor a single nanoscopic area while it is exposed to high energy oxygen, we have directly observed the growth of oxide islands with exposure to 1.2 eV O_2 impinging at a 45° angle (0.8 eV kinetic energy normal to the surface) as shown in Fig. 6, providing explicit evidence of the spatially heterogeneous oxidation mechanism. This figure illustrates representative examples of the spatially heterogeneous growth of patches of oxide in otherwise clean areas on the GaAs surface. Each set of images shows a single nanoscopic area as it is exposed to oxygen, demonstrating spatially heterogeneous oxide islands nucleating near defects and growing across the surface. There is a sharp divide between oxidized and unoxidized areas in these images, with the terraces not overtaken by oxide islands remaining clean. These images demonstrate conclusively that the heterogenous oxidation mechanism is activated at high oxygen energies, with oxide islands nucleating and growing laterally across the surface while surrounding areas remain unoxidized.

STM imaging with a variety of different surface bias values indicates that the observed elevation of the oxide islands is reflective of the surface topography, not electronic effects. The exact coordination of the chemisorbed oxygen atoms within the oxide cannot be determined by STM, but due to the inherent instability of the GaAs-As_2O_3 interface, the oxides are assumed to largely consist of Ga_2O_3 [51]. The observed spatial heterogeneity suggests that the activated dissociative chemisorption of the high kinetic energy O_2 is favored on intrinsic surface defect sites, consistent with previous findings [21,22]. Subsequent three-dimensional oxide growth might then occur at these nucleation sites, which would lead to the formation of the spatially heterogeneous oxide islands. The results of this study conclusively demonstrate the activation of a distinct heterogeneous oxidation process, adding to the knowledge base on the oxidation of this important electronic material.

Although heterogenous oxidation is the dominant mechanism at high oxygen kinetic energies, the homogenous mechanism was also found to occur simultaneously, indicating competition between the two mechanisms. Representative examples of a surface before and after exposure to normal-angle 1.0 eV O_2 are shown in Fig. 7, with the randomly distributed bright features corresponding to individual oxidized sites [36]. An analysis of the *x* and *y* coordinates of the bright protrusions in seven 40 nm × 40 nm images of a surface exposed to 4 × 10^{17} cm^2 of 1.0 eV oxygen, including the one shown in Fig. 7B, finds an average nearest neighbor separation of 2.2 ± 0.1 nm, which matches the separation of 2.2 ± 0.1 nm expected for a stochastic process once the presence of image boundaries is taken into consideration [52]. The density of oxidized sites grows linearly with exposure, as shown in Fig. 8 for exposure to 1.1 eV oxygen. The slope of this plot corresponds to the reaction probability of the homogenous mechanism at this oxygen kinetic energy. The linear trend therefore indicates a constant reaction probability with exposure, suggesting that in the low coverage limit, the homogeneous chemisorption of oxygen atoms to the GaAs(110) surface does not affect the subsequent reactivity of the surrounding surface sites. The spatially homogeneous oxidation mechanism therefore represents a stochastic process in the low coverage limit whereby oxygen molecules dissociatively chemisorb on unreacted surface sites with a constant reaction probability. The reaction probability of the homogeneous oxidation mechanism at higher coverages could not be measured due to the complete consumption of the surface in an oxide layer resulting from the kinetically dominant heterogeneous oxidation process.

Measurements of oxide formation with oxygen impinging normal to the GaAs(110) surface demonstrate that increasing O_2 kinetic energy greatly enhances the reactivity of both the spatially heterogeneous and homogeneous mechanisms of oxidation above the observed energy threshold of 0.7–1.0 eV. The comparative kinetics for the heterogeneous

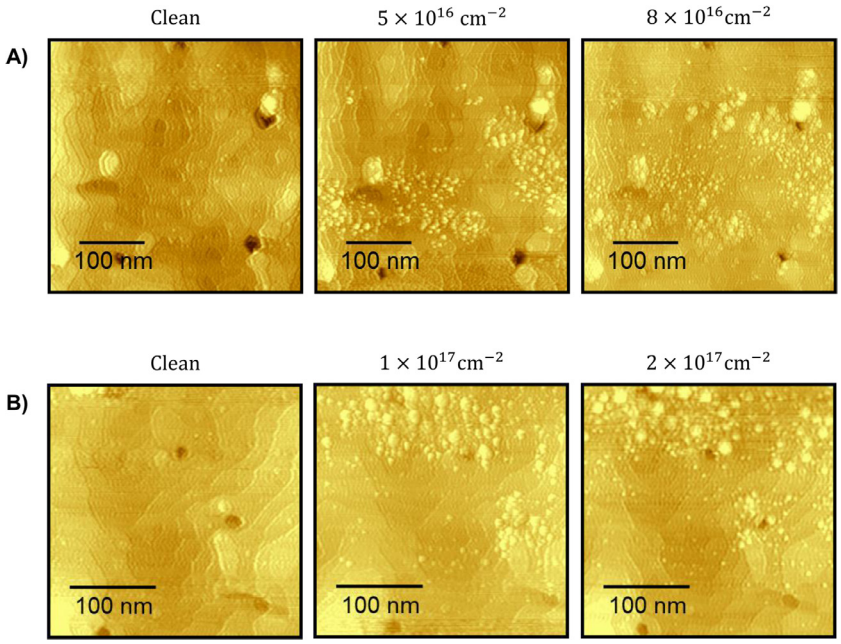

Fig. 6. Multiple examples of sequential STM images (−2.8 V, −0.6n A) in which the same local area is revisited after each exposure, directly demonstrating the growth of spatially heterogeneous oxide structures on a room temperature GaAs (110) surface with exposure to 1.2 eV O_2 impinging 45° from normal to the surface. Total exposures of O_2 are given above each STM image. **A)** A sequence of 400 nm × 400 nm images in a single area. **B)** A sequence of 300 nm × 300 nm images in another area with longer exposures. Both **A)** and **B)** demonstrate the emergence of spatially heterogeneous oxide patches (seen as clusters of large bright features on the surface) while nearby terraces remain largely unoxidized.

and homogeneous oxidation mechanisms are plotted in Fig. 9 for impinging O_2 energies from 1.0–1.2 eV; this plot demonstrates the strong correlation for both mechanisms between impinging O_2 kinetic energy and the reactivity of a room temperature GaAs(110) surface. The heterogeneous reaction probability was calculated indirectly by subtracting the contribution of the homogeneous mechanism from the overall reaction probability. The figure demonstrates that the fast kinetics of the heterogeneous mechanism completely dominate surface oxidation at O_2 kinetic energies ≥1.0 eV. The homogeneous oxidation reaction rate also increases with increasing O_2 kinetic energy, similar to the heterogeneous reaction rate, but the values for the reaction probability of the homogeneous mechanism at each energy are 3–4 orders of magnitude lower than those of the heterogeneous growth mechanism. The dominant oxidation mechanism at high oxygen energies is therefore the heterogenous nucleation of oxide islands on surface defects that grow laterally to consume the surface, outcompeting the homogenous accumulation of oxidized sites and subsequent layer-by-layer growth.

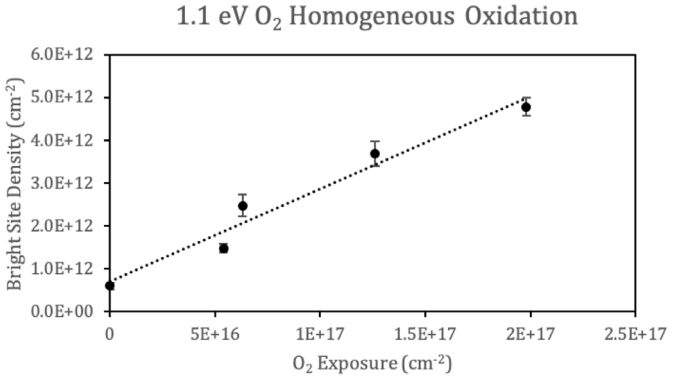

Fig. 8. A reactivity plot demonstrating the increasing areal density of homogeneous oxidation sites on a room temperature GaAs(110) surface after continued exposure to O_2 with a kinetic energy of 1.1 eV. The slope of the linear fit represents the probability of an O_2 molecule colliding with the GaAs(110) surface and forming an individual bright protrusion as imaged by STM. The linearity of the fit indicates that oxidized sites do not influence the reactivity of the surface to subsequent oxidation in the low coverage limit.

4. Conclusions

The results of this study demonstrate the enhanced oxidation of a room temperature GaAs(110) surface using impinging O_2 with high kinetic energies (≥1.0 eV), representing an enhanced method of oxidizing a GaAs surface at moderate temperatures. Surface dynamics and energetic dependencies at the atomic scale were examined by monitoring the *in-situ* evolution of the GaAs(110) surface during exposures to tightly controlled energy- and angle-selected O_2. Increasing the kinetic energy of the impinging O_2 dramatically increases the probability for dissociative chemisorption, while also markedly altering

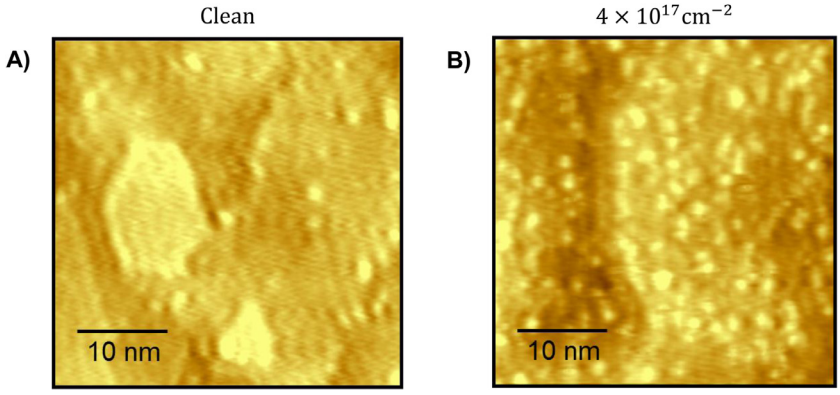

Fig. 7. STM images in different local areas of the surface, representative of the **A)** clean GaAs(110) surface (40 nm × 40 nm; −3.0 V, −0.6 nA) and **B)** a surface after exposure to ~4 × 10^{17} cm^{-2} of O_2 with a kinetic energy of 1.0 eV (40 nm × 40 nm, −2.0 V, −0.6 nA). Comparison of these two images demonstrates the difference in the density of chemisorbed oxygen atoms (the bright protrusions) before and after exposure to 1.0 eV O_2 as the surface undergoes homogeneous oxidation. The spacing between nearest neighbors matches that of a stochastic process, indicating that the presence of the oxidized sites does not significantly affect the reactivity of surrounding surface atoms.

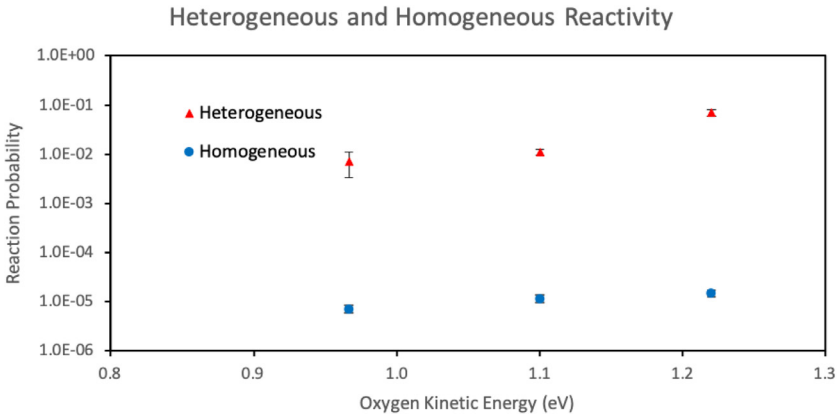

Fig. 9. A reactivity plot illustrating the O_2 impinging kinetic energy dependence of the reaction probabilities of the heterogeneous and homogeneous oxidation mechanisms on a room temperature GaAs(110) surface. The data show that the reactivities of both mechanisms increase with oxygen kinetic energy, and that the heterogeneous mechanism dominates over the homogenous mechanism at each energy. The reaction probability is plotted on a logarithmic scale on the y-axis, and is calculated as the ratio of the number of individual bright oxidized sites to the total number of O_2 collisions for the homogeneous mechanism, and as the ratio of the number of impinging O_2 molecules that contribute to a 10 Å thick oxide layer to the total fluence of O_2 molecules (minus the contribution of the homogeneous mechanism) for the heterogeneous mechanism.

the morphology of the resulting oxides. Oxidation proceeds through multiple competing mechanisms, with the dominant oxidation mechanism dependent upon the incident O_2 kinetic energy. While the homogenous mechanism with randomly distributed oxidized sites leading to layer-by-layer growth is expected to dominate at low oxygen kinetic energies, at high kinetic energies the heterogenous mechanism dominates, with oxide islands nucleating on surface defects and growing laterally and vertically. Results suggest that the oxide islands can be physically uplifted by subsurface oxidation that nucleates at defect sites and induces lattice expansion that forces the surface to grow vertically in a "blistering" fashion. Homogeneous oxidation was observed occurring simultaneously but at a lower rate, resulting in the domination of the heterogeneous mechanism. The heterogeneous formation and growth of oxide islands was observed at all impinging O_2 kinetic energies at or above 1.0 eV, with the reaction probabilities of both mechanisms increasing with oxygen kinetic energy. The results of this study reveal spatio-temporal correlations that link the varying oxidation kinetics on the GaAs(110) surface to specific surface morphologies on a broad range of length scales. This provides new insight into the initial oxidation stages of GaAs surfaces that is vital to better controlling oxidation during material processing, represents a possible method of creating crucial ultra-thin oxide films with enhanced efficiency at lower surface temperatures, and offers a potential route to enabling a high degree of interfacial abruptness. A greater understanding of the dynamics of GaAs oxidation holds the potential for new techniques allowing passivation and modification of GaAs at moderate surface temperatures for the effective manufacturing and optimal functioning of this high-performance semiconductor.

CRediT authorship contribution statement

Tim Grabnic: Conceptualization, Formal analysis. **Ross Edel:** Conceptualization, Formal analysis. **S.J. Sibener:** Conceptualization, Formal analysis.

Acknowledgment

This work was supported by the National Science Foundation, Grant no. CHE-1900188 with focus on spatio-temporal interfacial reaction kinetics, and by the Air Force Office of Scientific Research, Grant no. FA9550-19-1-0324. Support from the NSF-Materials Research Science and Engineering Center at the University of Chicago, Grant no. NSF-DMR-14-20709, is also gratefully acknowledged. The authors thank Michelle Brann and Rebecca Thompson for technical assistance.

References

[1] J.A. del Alamo, Nanometre-scale electronics with III–V compound semiconductors, Nature 479 (2011) 317–323.
[2] L. G.M. Whitesides, Materials for advanced electronic devices, in: M. Good, R. Baum, I. Peterson, N. Henderson (Eds.), Biotechnology and Materials Science: Chemistry for the Future, American Chemical Society, Washington, DC, 1988, pp. 85–99.
[3] P. Schmuki, G.I. Sproule, J.A. Bardwell, Z.H. Lu, M.J. Graham, Thin anodic oxides formed on GaAs in aqueous solutions, J. Appl. Phys. 79 (1996) 7303–7311.
[4] H.-.H. Wang, J.-.Y. Wu, Y.-.H. Wang, M.-.P. Houng, Effects of pH values on the kinetics of liquid-phase chemical-enhanced oxidation of GaAs, J. Electrochem. Soc. 146 (1999) 2328–2332.
[5] M. Telford, Progress in GaAs manufacturing technology, III-vs review14 (2001) 22–26.
[6] A. Pakes, P. Skeldon, G.E. Thompson, R.J. Hussey, S. Moisa, G.I. Sproule, D. Landheer, M.J. Graham, Composition and growth of anodic and thermal oxides on INP and GaAs, Surf. Interface Anal. 34 (2002) 481–484.
[7] H.-.Y. Lee, Growth of GaAs oxide layer using photoelectrochemical method, J. Electrochem. Soc. 155 (2008) G141.
[8] H.-.Y. Lee, Y.-.F. Lin, GaAs metal-oxide-semiconductor devices with a complex gate oxide composed of SiO_2 and GaAs oxide grown using a photoelectrochemical oxidation method, Semicond. Sci. Technol. 25 (2009) 015005.
[9] F. Gucmann, R. Kúdela, P. Kordoš, E. Dobročka, Š. Gaži, J. Dérer, J. Liday, P. Vogrinčič, D. Gregušová, III-As heterostructure field-effect transistors with recessed ex-situ gate oxide by O2 plasma-oxidized GaAs cap, J. Vac. Sci. Technol. B 33 (2015) 01A111.
[10] H. Sharma, K. Moumanis, J.J. Dubowski, pH-Dependent photocorrosion of GaAs/AlGaAs quantum well microstructures, J. Phys. Chem. C 120 (2016) 26129–26137.
[11] K.D. Childs, M.G. Lagally, Species-specific densities of states of Ga and As in the chemisorption of oxygen on GaAs(110), Phys. Rev. B 30 (1984) 5742–5752.
[12] W. Mönch, Oxidation of silicon and III–V compound semiconductors, in: W. Mönch (Ed.), Semiconductor Surfaces and Interfaces, Springer, Berlin Heidelberg, 2001, pp. 353–376.
[13] B. Wiggins, L.G. Avila-Bront, R. Edel, S.J. Sibener, Temporally and spatially resolved oxidation of si(111)-(7 × 7) using kinetic energy controlled supersonic beams in combination with scanning tunneling microscopy, J. Phys. Chem. C 120 (2016) 8191–8197.
[14] R. Edel, T. Grabnic, B. Wiggins, S.J. Sibener, Atomically-Resolved oxidative erosion and ablation of basal plane HOPG graphite using supersonic beams of O_2 with scanning tunneling microscopy visualization, J. Phys. Chem. C 122 (2018) 14706–14713.
[15] D.J. Frankel, J.R. Anderson, G.J. Lapeyre, UV photoemission study of low temperature oxygen adsorption on GaAs(110), J. Vac. Sci. Technol. B 1 (1983) 763–766.
[16] F. Bartels, L. Surkamp, H.J. Clemens, W. Mönch, Oxygen and hydrogen adsorption on GaAs(110), J. Vac. Sci. Technol. B 1 (1983) 756–762.
[17] G. Hughes, R. Ludeke, O 1s studies of the oxidation of InP(110) and GaAs(110) surfaces, J. Vac. Sci. Technol. B 4 (1986) 1109–1114.
[18] W. Mönch, On the oxidation of III–V compound semiconductors, Surf. Sci. 168 (1986) 577–593.
[19] F. Bartels, W. Mönch, On the growth mode of oxide films on cleaved GaAs(110) surfaces at room temperature, Solid State Commun. 57 (1986) 571–574.
[20] F. Bartels, W. Mönch, Oxidation mechanism of III–V semiconductors, Vacuum 41 (1990) 667–668.
[21] G. Landgren, R. Ludeke, Y. Jugnet, J.F. Morar, F.J. Himpsel, The oxidation of GaAs (110): a reevaluation, J. Vac. Sci. Technol. B 2 (1984) 351–358.
[22] G. Landgren, R. Ludeke, J.F. Morar, Y. Jugnet, F.J. Himpsel, Oxidation of GaAs (110): new results and models, Phys. Rev. B 30 (1984) 4839–4841.
[23] K.A. Bertness, J.-.J. Yeh, D.J. Friedman, P.H. Mahowald, A.K. Wahi, T. Kendelewicz, I. Lindau, W.E. Spicer, Growth structure of chemisorbed oxygen on GaAs(110) and InP(110) surfaces, Phys. Rev. B 38 (1988) 5406–5421.
[24] N. Cabrera, N.F. Mott, Theory of the oxidation of metals, Rep. Prog. Phys. 12 (1949) 163–184.
[25] P. Pianetta, I. Lindau, C.M. Garner, W.E. Spicer, Oxidation properties of GaAs (110) surfaces, Phys. Rev. Lett. 37 (1976) 1166–1169.
[26] P. Pianetta, I. Lindau, C. Garner, W.E. Spicer, Determination of the oxygen binding site on GaAs(110) using soft-x-ray-photoemission spectroscopy, Phys. Rev. Lett. 35

(1975) 1356–1359.
[27] P. Pianetta, I. Lindau, C.M. Garner, W.E. Spicer, Chemisorption and oxidation studies of the (110) surfaces of GaAs, GaSb, and InP, Phys. Rev. B 18 (1978) 2792–2806.
[28] R. Ludeke, The oxidation of the GaAs (110) surface, Solid State Commun. 21 (1977) 815–818.
[29] R. Ludeke, Oxidation properties of GaAs (110) surfaces, Phys. Rev. B 16 (1977) 5598–5599.
[30] C.R. Brundle, D. Seybold, Oxygen interaction with GaAs surfaces: an XPS/UPS study, J. Vac. Sci. Technol. 16 (1979) 1186–1190.
[31] M.-.H. Tsai, W.E. Packard, J.D. Dow, R.V. Kasowski, Oxidation of the GaaS(110) surface, Physica B 192 (1993) 365–370.
[32] W.E. Spicer, I. Lindau, P.E. Gregory, C.M. Garner, P. Pianetta, P.W. Chye, Synchrotron radiation studies of electronic structure and surface chemistry of GaAs, GaSb, and InP, J. Vac. Sci. Technol. 13 (1976) 780–785.
[33] R. Dorn, H. Lüth, G.J. Russell, Adsorption of oxygen on clean cleaved (110) gallium-arsenide surfaces, Phys. Rev. B 10 (1974) 5049–5056.
[34] P.W. Chye, P. Pianetta, I. Lindau, W.E. Spicer, Oxygen sorption and excitonic effects on GaAs surfaces, J. Vac. Sci. Technol. 14 (1977) 917–919.
[35] R. Ludeke, A. Koma, Electronic surface states on clean and oxygen-exposed GaAs surfaces, J. Vac. Sci. Technol. 13 (1976) 241–247.
[36] J.A. Stroscio, R.M. Feenstra, A.P. Fein, Structure of oxygen adsorbed on the GaAs (110) surface studied using scanning tunneling microscopy, Phys. Rev. B 36 (1987) 7718–7721.
[37] P. Kruse, J.G. McLean, A.C. Kummel, Relative reactivity of arsenic and gallium dimers and backbonds during the adsorption of molecular oxygen on GaAs(100) (6×6), J. Chem. Phys. 113 (2000) 9217–9223.
[38] P. Kruse, J.G. McLean, A.C. Kummel, Chemically selective adsorption of molecular oxygen on GaAs(100)c(2×8), J. Chem. Phys. 113 (2000) 9224–9232.
[39] M. Passlack, M. Hong, J.P. Mannaerts, R.L. Opila, F. Ren, Thermodynamic and photochemical stability of low interface state density Ga_2O_3–GaAs structures fabricated by in situ molecular beam epitaxy, Appl. Phys. Lett. 69 (1996) 302–304.
[40] R.M. Feenstra, J.A. Stroscio, J. Tersoff, A.P. Fein, Atom-selective imaging of the GaAs(110) surface, Phys. Rev. Lett. 58 (1987) 1192–1195.
[41] J.A. Stroscio, R.M. Feenstra, A.P. Fein, Local state density and long-range screening of adsorbed oxygen atoms on the GaAs(110) surface, Phys. Rev. Lett. 58 (1987) 1668–1671.
[42] P. Moriarty, G. Hughes, An investigation of the early stages of native oxide growth on chemically etched and sulfur-treated GaAs(100) and InP(100) surfaces by scanning tunnelling microscopy, Ultramicroscopy 42–44 (1992) 956–961.
[43] I. Nevo, S. Aloni, S.R. Cohen, G. Hasse, The effect of adsorbed oxygen on the surface potential of n-GaAs(110), J. Chem. Phys. 123 (2005) 064705.
[44] G. Hollinger, G. Hughes, F.J. Himpsel, J.L. Jordan, J.F. Morar, F. Houzay, Early stages in the formation of the oxide-InP(110) interface, Surf. Sci. 168 (1986) 617–625.
[45] D.A. King, M.G. Wells, Molecular beam investigation of adsorption kinetics on bulk metal targets: nitrogen on tungsten, Surf. Sci. 29 (1972) 454–482.
[46] P. Piercy, A.M.-J. Castonguay, Diffusion-limited kinetics of terrace growth on GaAs (110), Phys. Rev. B (2005) 72.
[47] R.J. Pechman, X.-.S. Wang, J.H. Weaver, Vacancy kinetics and sputtering of GaAs (110), Phys. Rev. B 51 (1995) 10929–10936.
[48] X.-.S. Wang, R.J. Pechman, J.H. Weaver, Trends in surface roughening: analysis of ion-sputtered GaAs(110), Surf. Sci. 364 (1996) L511–L518.
[49] N.T. Barrett, G.N. Greaves, S. Pizzini, K.J. Roberts, The local atomic structure of the oxide coating on polished GaAs(100), Surf. Sci. 227 (1990) 337–346.
[50] M.G. Proietti, J. Garcia, J. Chaboy, F. Morier-Genoud, D. Martin, Structural properties of GaAs oxide layers grown on polished (100) surfaces, J. Phys. 5 (1993) 1229–1238.
[51] C.D. Thurmond, G.P. Schwartz, G.W. Kammlott, B. Schwartz, GaAs oxidation and the GaAsO equilibrium phase diagram, J. Electrochem. Soc. 127 (1980) 1366–1371.
[52] K. Donnelly, Simulations to determine the variance and edge-effect of total nearest neighbour distance, in: I. Hodder (Ed.), Simulation Methods in Archaeology, Cambridge University Press, London, 1978, pp. 91–95.